Conf-910640--25

SAND--90-3020C

DE91 014662

Received

JUL 0 2 1991

EXPERIMENTAL AND ANALYTICAL STUDY OF LASER-TRIGGERING IN THE RIMFIRE SWITCH*

B. N. Turman
Sandia National Laboratories
P. O. Box 5800
Albuquerque, NM 87185

A. E. Rodriguez and K. J. Touryan
Tetra Corporation
4509 Hawkins NE
Albuquerque, NM 87109

Abstract

The Rimfire multi-stage gas switch is a low-jitter switch that was developed to meet high-voltage and low-jitter requirements for the PBFA-II pulsed power accelerator. The first stage is laser-triggered. Streak and framing camera data have been collected to determine the closure time, jitter, and optimum parameters for laser triggering. Three phases of closure are observed: (1) fast discharge phase, (2) channel heating phase, and (3) current conduction phase. Gap closure time and jitter are measured as a function of voltage, laser energy, and focal position. A computer model has been developed with sufficient physics detail to provide good agreement with these data. SF_6 Boltzmann kinetics, multi-photon laser ionization, and photodetachment are included. The photodetachment rate is shown to be a critical parameter in determining the minimum trigger energy for an undervolted SF_6 gap. The model gives good agreement with experimental closure times and minimum laser energy requirements.

I. Introduction

The PBFA II rimfire switch[1] is shown in Fig. 1. The switch has a laser-triggered first stage, to take advantage of the low jitter capability demonstrated by previous laser triggering experiments[2, 3]. A KrF beam is focused within the trigger gap, which is shown on the right-hand side of Fig. 1. Subsequent stages are self-fired from the overvoltage of the closed trigger stage. The runtime of the switch is dependent on pressure and voltage and is in the range of 20-60 ns. Experiments have shown that the major timing dependence comes from the trigger stage, since the remaining stages are so highly overvolted upon closure.

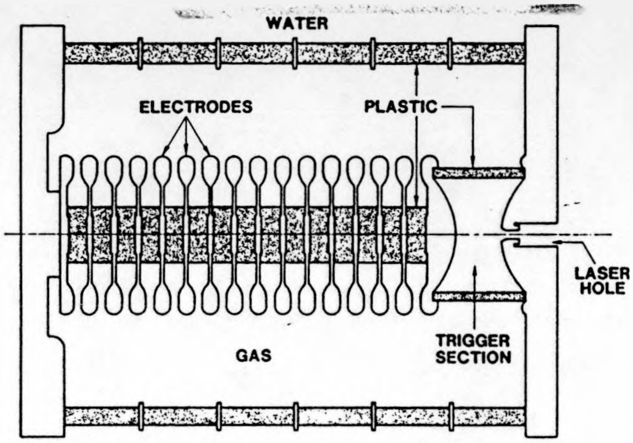

Figure 1. Schematic of the PBFA Rimfire switch.

This paper will report results from experiments designed to study the triggering mechanisms and timing variability of the laser-triggered first stage. A computer model has been developed to give additional physical insight, and allow extrapolations from these experiments. The computer model is based on Boltzmann calculations of electron transport and kinetic rate coefficients, thermal ionization in the heating phase of the developing arc, photodetachment, and multi-photon laser ionization.

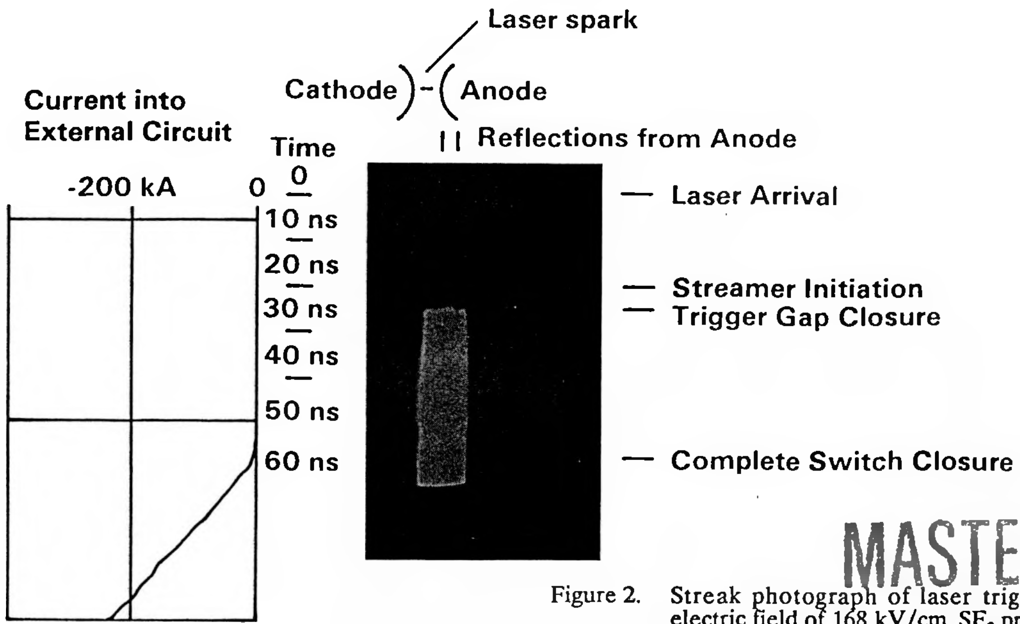

Figure 2. Streak photograph of laser triggered gap, at an electric field of 168 kV/cm, SF_6 pressure of 4.8 bars, laser energy of 16 mJ. A neutral density filter of 0.7 ND attenuates the initial laser spark intensity below the camera threshold, and the channel becomes visible only after the trigger gap is closed.

*This research was funded under DOE Contract Number DE-AC04-76DP00789.

II. Laser Triggered Gap Closure Observations

These experiments have been conducted with laser energy of 5 to 60 mJ, in a pulse of 22 ns FWHM. A visible spark is formed in the gap at the plane where the laser power density exceeds the gas breakdown threshold (5 x 10^9 watts/cm^2 at 3 bars [4]). The length of this spark is determined by the convergence angle and the power density of the laser beam. Under these conditions, the visible plasma channel created by the laser spark is up to 2 cm in length, or about half the gap length. Simple models developed by Morrow[5] and Martin[6] predict that the gap therefore should be triggerable down to about half of the self-breakdown voltage. That prediction is confirmed by these experiments.

A streak camera and gated imaging camera were triggered and synchronized with the laser trigger through a CAMAC-based timing system. This arrangement allowed accurate measurement of time delays for the trigger stage and each subsequent stage. The threshold sensitivity of the gated imaging camera was estimated by observing low-level emission from a light-emitting diode (640 nm) and measuring the intensity of the source with a calibrated optical power meter. The gated camera threshold was about 3 x 10^{-11} J per picture element, or about 0.4 μJ of energy radiated from a (0.5 mm)^3 source at 3-m distance. Concurrent observation of the laser spark was used to estimate the streak camera threshold. With a ND 0.7 neutral density filter, as normally used in the experiment, the streak camera threshold was about 80 watts from a (0.5 mm)^3 source at 3-m distance. The sensitivities of the two cameras are approximately the same for an event time scale of 5 ns.

Figure 2 shows a typical streak photograph of the early phases of gap triggering, where the laser spark is focused in the middle of the gap. Three distinct phases are observable: (1) a dim early phase in which a fast discharge appears within a few nanoseconds after the arrival of the laser spark, (2) a brighter phase in which the laser spark becomes visible and the entire channel heats, (3) the current-carrying phase in which the current transferred through the switch heats the gap rapidly to a high conductivity and final breakdown. This sequence has been postulated by Martin[6] as a general feature of gap breakdown.

The onset of the fast discharge occurs soon after the beginning of the laser trigger pulse. Figure 2 shows that optical emission is observed within 20 ns of the start of the laser pulse, for the triggering condition of Fig. 2. Trigger arrival time is defined by the timing threshold setting of approximately 5% of the peak laser intensity. As can be noted from Fig. 2, the initial radiation is not uniform across the length of the gap; the region of the triggering laser spark (about 2 cm length in this photo) is much more intense than the remainder of the gap. The onset time of the fast discharge is dependent on voltage, laser energy, and spark location. The delay between the fast discharge and channel completion is approximately constant, at 2 ns.

Sequential gated photographs of the trigger gap closure are shown in Fig. 3. These photographs were taken on successive shots, with the camera gate changed to observe longer integration times on each shot. These photos show that the discharge develops along the axis, and the channel moves away from the axis only near the laser entry hole on the anode.

The closure time of the trigger section was measured from streak camera records. Current and voltage measurements on both the intermediate store and line 1 monitors (upstream and downstream of the switch) indicate that a weak current begins to flow from the entire switch at the time that anode and cathode streamers connect to the laser spark. A sudden brightening of the laser spark occurs at that time also, as seen from Fig. 2. The sudden brightening of the laser spark is therefore used to define the closure time of the trigger gap.

Figures 4, 5, and 6 show the dependence of trigger gap closure time on the laser energy and the axial position of the laser spark within the gap. Figure 4 gives the laser energy dependence, at 53% self-break voltage and the laser spark at

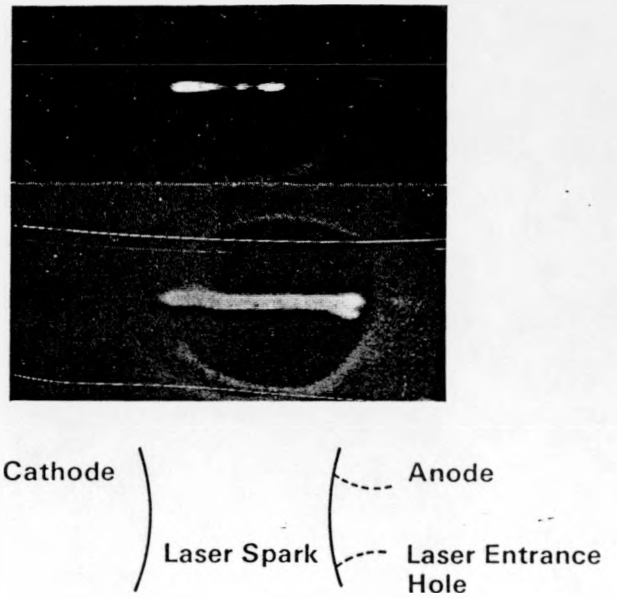

Figure 3. Gated camera photos of the trigger gap closure sequence. Laser energy is 16 mJ, with the Laser spark centered in the gap. Cathode electrode is to the left, anode to the right. Gap spacing is 4.5 cm., electric field is 190 kV/cm, pressure is 4.8 bars. Camera shutter closed 26 ns after laser arrival in (a), 36 ns in (b).

the center of the gap. The jitter of the trigger gap is also plotted. Note that jitter increases substantially when the gap closure time becomes longer than the laser pulse width of 22 ns FWHM. Figure 5 gives trigger gap closure times for several laser energy values, plotted against switch voltage. Closure time can be fitted by the formula:

$$t_t = \frac{e_o}{P}(1-\upsilon) \qquad (1)$$

where e = 0.03 J, a threshold laser energy, P is the average input laser power in watts, υ is fraction of self-break voltage, and t_t is the closure time in seconds.

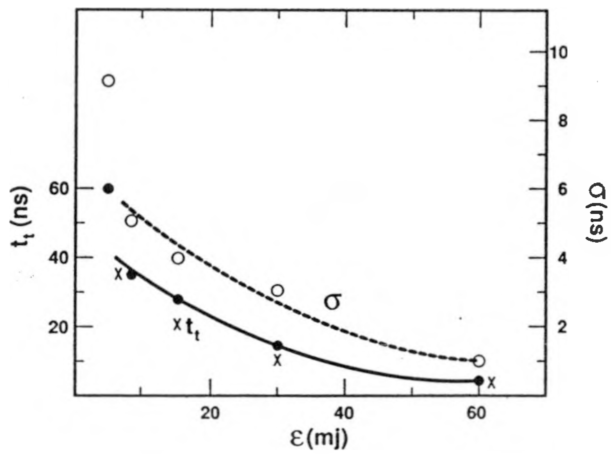

Figure 4. Trigger section closure time (dots) and jitter (circles) vs. laser energy at 53% of self-break voltage. The laser spark is centered in the trigger gap. X indicates calculated closure times.

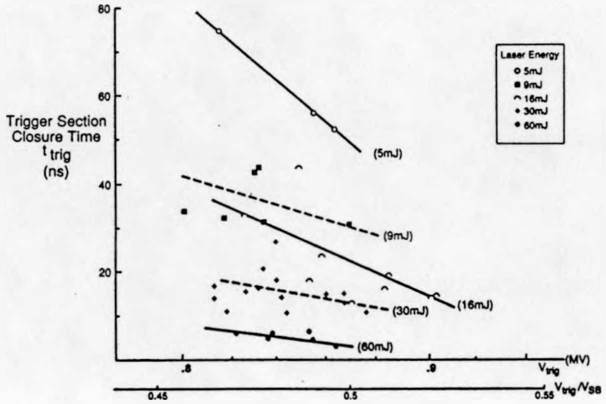

Figure 5. Trigger section closure vs. switch voltage at trigger.

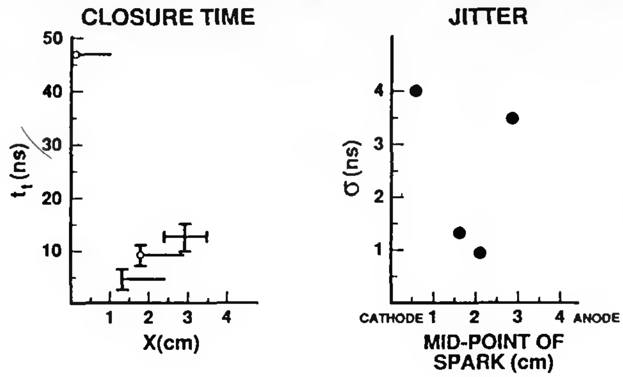

Figure 6. Trigger section closure time and jitter vs. spark position at 60 mJ laser energy and 53% of self-break voltage.

Figure 6 shows a broad minimum in closure time when the laser spark is focused at the center of the gap. Within ± 0.5 cm of the center, the run time changes by no more than 4 ns. As the spark is moved toward either electrode, the closure time and jitter increase. When the closure time becomes longer than the laser pulse width, the jitter generally increases, as the cathode-focused data point in Figure 6 indicates. Why the closure time is so long here is not clear, but we may have inadvertently shortened the laser spark length at the cathode by focusing it too near the cathode surface. The jitter for the anode-focused data point is also high. In this case, the large jitter may be partially due to the fact that the laser spark is near the 1 cm-diameter laser entrance hole, and sideward-connection of the discharge becomes problematic.

III. Laser Triggered Spark Gap Modeling

A model has been developed for studying laser triggering of SF_6 spark gaps[7,8,9]. The modeling starts with an examination of the basic kinetics of SF_6-cross-section data in a Boltzmann code to calculate electron transport and kinetic rate coefficients. To these data is added a model of thermal ionization capable of breaking down the normal gas resistance to conduction, following a heating phase which dominates the breakdown time. The strong SF_6 attachment is kept from quenching this intermediate glow discharge only by photodetachment, induced by the laser.

Next, the laser interactions are modeled, starting with a simple focused beam geometry. The laser/SF_6 interaction is dominated by 2-photon excitation of the 10 eV metastable state, followed by 2-photon ionization of the excited population. Nonlinear laser absorption is discernible, but not dominant.

Finally, the laser ionization model is incorporated into a quasi-2D streamer code. The basis of the streamer code includes the quasi-2D space-charge field calculation, flux-corrected transport and solution-adapted 1D grid. The output includes plots at various simulations times of electron and ion densities, net charge density and total electric field, and animations of streamer development and propagation.

IV. Modeling Results

The first tests of the validity of the modeling can be applied by comparing with experimental data concerning the minimum laser energy requirement and the minimum voltage for triggering. Figure 4 shows that the minimum laser energy for triggering a gap at 53% self-break voltage is about 10 mJ (the energy required to close the gap within the 22 ns pulse duration of the laser, and with jitter of less than 4 ns).

The intense laser radiation of the focused beam interacts with the SF_6 molecules through two principal mechanisms: multiphoton ionization and photodetachment. In an undervolted SF_6 gap, particularly at 50% of self-break, calculations show the electron attachment rate of SF_6 dominates the photo- and Townsend-ionization rates of the focused laser beam for moderate energy. The photodetachment process, in which UV photons detach electrons from negative ions, competes with attachment. The calculations show that SF_6 photodetachment rate and SF_6 attachment rate for these laser triggering conditions are comparable. Figure 7 shows the calculated equilibrium density for a 5 mJ focused laser beam in a gap at 75% self-break, or about 66 kV/cm. Figure 8 shows the result of Boltzmann analysis for this case. Note that the equilibrium electron density achieves a steady-state of about 10^{16} cm^{-3}, through the balance of photoionization and Townsend ionization, attachment, and photodetachment. The temperature increases through ohmic heating, reaching 10,000° K at 60 ns. At this temperature, thermal ionization becomes significant. The electron density and temperature rise abruptly in a non-linear coupling and the gap "closes."

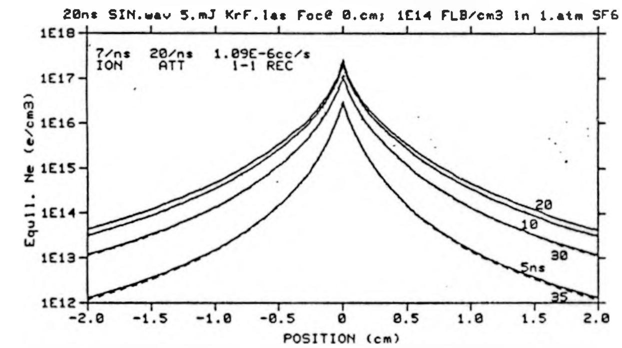

Figure 7. Equilibrium electron density profiles for 5 mJ laser energy.

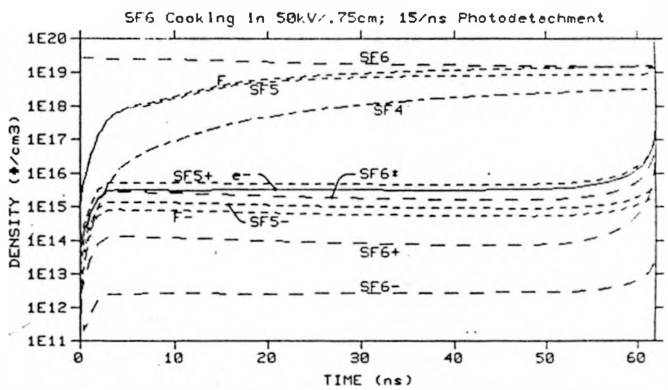

Figure 8. Species number density histories for nominal case (see text). (15/ns Photodetach rate corresponds to 5 mJ laser pulse.)

Gap closure time, as calculated from the Boltzmann kinetics model is plotted in Figure 4 for comparison with data. Note that 5 mJ and 60 mJ calculations agree well with measurements, and intermediate energy values agree within about 50%.

Is there an optimum laser pulse shape that would give the best energy efficiency for triggering the gap? Intuitively, one might suspect that a square wave shape would give the best efficiency, since this shape would maximize the intensity, I. The two-photon photoionization rate scales as I^2, but the photodetachment scales linearly. Since photodetachment plays a strong role, the net effect seems to be essentially independent of intensity, a function primarily of the total input energy. The square-wave and sinusoidal wave shapes were compared with 5 mJ and 60 mJ simulations with a 20 ns FWHM sine wave and a 20 ns square pulse. The simulations show that the square pulse gives only a slight increase of about 20% improvement in the integrated electron density. Experiments had shown no clear evidence of a strong dependence on laser power, but primarily laser energy.

V. Summary

These experiments have measured the closure time-voltage behavior of the laser-triggered spark gap, determined closure time and jitter as a function of laser energy, and observed the sensitivity of closure time to position within the gap. A computer model has been developed to provide physical insight and engineering modeling capability. The model is based on photoionization and photodetachment, Townsend ionization, and electron attachment rates combined in a Boltzmann statistics model. Good agreement is obtained between the experiment and model.

References

[1] B. N. Turman, D. R. Humphreys, and C. N. Richards, "Interstage Closure Times for the Rimfire Multistage Gas Switch," Proceedings of the 7th IEEE Pulsed Power Conference, Monterey, CA, 1989, pp. 555=558.

[2] A. H. Guenther & J. R. Bettis, "The Laser Triggering of High-Voltage Switches," J. Phys. D: Appl. Phys., Vol. 11, 1577, 1978.

[3] J. R. Woodworth, P. J. Harjes, L. C. Pitchford, and R. A. Hamil, "Laser Triggering of a 500-kV Gas-Filled Switch: A Parametric Study," J. Appl. Phys., 56 p. 1382, 1984.

[4] W. R. Rapoport, "KrF Laser Triggered SF_6 Spark Gap for Low Jitter Timing," IEEE Trans. on Plasma Science, PS8, 167-170, 1980.

[5] Morrow, R., "Properties of Streamers and Streamer Channels in SF_6," Physical Review A, 35, No. 4, 1778, 1987.

[6] T. H. Martin, "An Empirical Formula for Gas Switch Breakdown Delay," Proceedings of the 7th IEEE Pulsed Power Conference, Monterey, CA, 1989, pp. 73-79.

[7] Rodriguez, et al., "Laser Triggered Spark Gap Modeling Final Report," Sandia National Laboratories Contractor Report SAND91-7065, Aug. 1990.

[8] Rodriguez, et al., "Modeling of a KrF Laser-Triggered Spark Gap," This Proceedings.

[9] A. E. Rodriguez, W. L. Morgan, K. J. Touryan, M. W. Moeny, and T. H. Martin, "An Air Breakdown Kinetic Model," to be published, J. Appl. Phys., Aug. 15, 1991.